JNC TN9400 2002-069

Physical and chemical properties of sodium ferrates and equilibrium calculations in H_2O/CO_2 environments

January 2003

OARAI ENGINEERING CENTER
JAPAN NUCLEAR CYCLE DEVELOPMENT INSTITUTE

〒319-1184　茨城県那珂郡東海村村松４番地49
核燃料サイクル開発機構
技術展開部　技術協力課

JNC TN9400 2002-069
2003年 1月

Physical and chemical properties of sodium ferrates and equilibrium calculations in H_2O/CO_2 environment

Jintao HUANG*, Tomohiro Furukawa* and Kazumi Aoto*

Abstract

Thermodynamic data for most of the Na-Fe oxides with Fe^{+2} and Fe^{+3} have been evaluated in previous studies by the present authors; however, crystal structure and thermodynamic data of $Na_4Fe_6O_{11}$ (or $Na_2O1.5Fe_2O_3$) have seldom been studied experimentally. To investigate its role in the Na-Fe-O system, sample $Na_4Fe_6O_{11}$ was prepared by heating $2Na_2CO_3+3Fe_2O_3$. The X-ray powder diffraction data of $Na_4Fe_6O_{11}$ were indexed by a monoclinic system with the cell parameters a=13.4622Å, b=5.3886Å, c=9.1317Å, α=90°, β=96.35°, γ=90.0°. By using Knudsen effusion mass spectrometry, the temperature dependence of CO_2 partial pressure over the mixture $2Na_2CO_3+3Fe_2O_3$ was determined as $\ln\{p(CO_2)/Pa\}=29.4385-29015.4/T$ (913-1023K). Thermodynamic data of $Na_4Fe_6O_{11}$ were then evaluated as, $\Delta_fH°(298.15K)$= -3569.54 ± 3.95 kJ·mol^{-1}, $\Delta_fG°(T)$ /J·mol^{-1} = $(-3716839 \pm 2274.55) + (1200.16 \pm 2.35) \times T/K$, $\Delta_fG°(298)$ is recommended as -3255.3 ± 12.4 kJ·mol^{-1}. It is further found that $Na_4Fe_6O_{11}$ is thermodynamically stable only at high temperatures over about 1200K. At lower temperatures, it tends to decompose into $NaFeO_2$ and $Na_5Fe_3O_9$.

A user database of the Na-Fe-O-H-C system was created so that equilibrium states of sodium ferrates in H_2O/CO_2 environments were calculated. Chemical potential diagrams as functions of P_{O2} and P_{Na} were constructed by Thermo-Calc. The simulation calculation suggested that $NaFeO_2$ should be the most stable sodium ferrite together with NaOH or Na_2CO_3 depending on the atmosphere, while other sodium ferrites such as Na_5FeO_4, Na_3FeO_3 etc...would be thermodynamically unstable. However, experiments by gas-inlet KEMS showed that the reaction rate of sodium ferrates with CO_2 was a time-consuming process. It indicates that reaction kinetics would play a great role in chemical behaviors of sodium ferrates in H_2O/CO_2 environments.

* Advanced Material Research Group, Advanced Technology Division,
O-arai Engineering Center

JNC TN9400 2002-069
January, 2003

ナトリウム鉄酸化物の物理化学特性及び水蒸気・CO_2雰囲気における平衡計算

黄錦涛*、古川智弘*、青砥紀身*

要　旨

二価および三価のナトリウムを含有する主要な鉄酸化物の熱力学データについて、著者らはこれまでに研究を実施してきた。本研究では、まだ着手していなかった三価の鉄酸化物、$Na_4Fe_6O_{11}$(または，$Na_2O1.5Fe_2O_3$)の結晶構造や熱力学的な研究を行った。同化合物は、Na_2CO_3とFe_2O_3を2：3に調合、高温加熱して作製した。X線回折パターンから、同化合物は単斜晶系構造（a=13.4622Å、b=5.3886Å、c=9.1317Å、α=90°、β=96.35°、γ=90°）であると推定された。高温質量分析法により、この化合物が合成されるときに放出されるCO_2ガスの圧力（CO_2分圧）の温度依存性を測定し、

$\ln p(CO_2)/Pa=29.4385-29015.4/T(913\text{-}1023K)$

が得られた。そしてこの結果を用いて$Na_4Fe_6O_{11}$の熱力学データについて以下のように定めた。

$\Delta_f H°(298.15K)= -3569.6\pm3.95$ kJmol^{-1}
$\Delta_f G°(T)$ /Jmol^{-1} = (−3716839 ± 2274.55) + (1200.16 ± 2.35) ×T/K
$\Delta_f G°(298)=-3255.3\pm12.4$ kJmol^{-1}

これまでに得られた各種のNaFe複合酸化物の熱力学データを活用して$Na_4Fe_6O_{11}$の安定性について調べたところ、およそ1270K以上の高温でなければ、同化合物は熱力学的に安定に存在し得ないことが得られた。また、これ以下の温度域では$Na_5Fe_3O_9$と$NaFeO_2$に分解する傾向がある．

このNaFe複合酸化物の熱力学データを用いて，H_2O/CO_2環境におけるナトリウム鉄酸塩の平衡状態を計算できるようにし、P_{O2}とP_{Na}の関数として化学ポテンシャル図を作成した。シミュレーション計算により，水蒸気と二酸化炭素を含む大気環境下では、NaOHまたはNa_2CO_3ともに、$NaFeO_2$が安定なナトリウム鉄酸塩として存在する（Na_5FeO_4やNa_3FeO_3等他のナトリウムフェライトは安定していない）ことが示された。しかしながら、ガス導入型高温質量分析計による実験では，CO_2とナトリウム鉄酸塩との反応速度が異常に低いことを示した。反応動力学の課題が、H_2O/CO_2環境においてNa-Fe酸化物の形態評価に重要であることが判明した。

*大洗工学センター　要素技術開発部　新材料研究グループ

Contents

List of tables

List of figures

Physical and chemical properties of sodium ferrates and equilibrium calculations in H_2O/CO_2 environment

1. Introduction

Transition metal Fe possesses multi oxidation states of Fe^{+2}, Fe^{+3}, Fe^{+4},and Fe^{+6} in the solid state, so that it can form various complex compounds with alkaline metals. In Na-Fe-O system, about 20 kinds of sodium ferrates [1-2] have been reported in literatures (Fig.1). Among them, those oxides with unusual high oxidation states such as iron valence over +4 are not stable and tend to decompose to its lower valence states [3]. Sodium ferrites with Fe^{+3}, such as $NaFeO_2$, Na_3FeO_3, Na_5FeO_4, $Na_8Fe_2O_7$, $Na_3Fe_5O_9$ as well as $Na_4Fe_6O_{11}$ are probably the most commonly found in nature. Though thermodynamic data for most of the Na-Fe oxides with Fe^{+2} and Fe^{+3} have been evaluated in previous studies [4,5], thermodynamic data of $Na_4Fe_6O_{11}$ has seldom been measured experimentally till now.

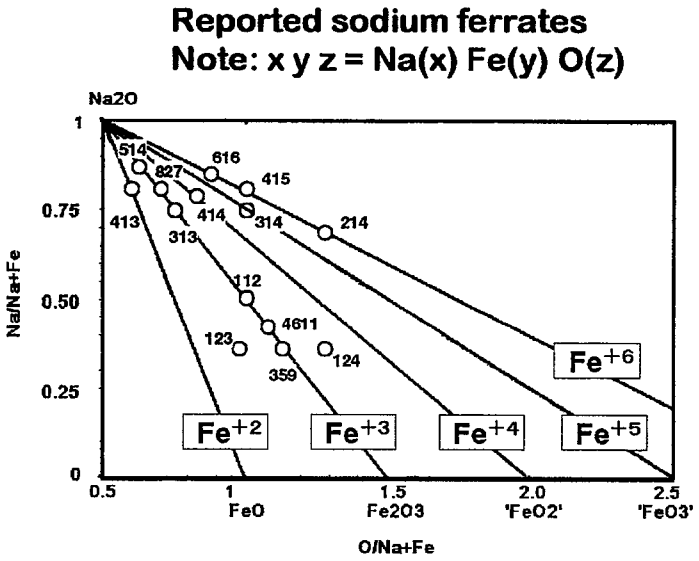

Fig. 1: Sodium ferrates reported in literatures

Sodium ferrite $Na_4Fe_6O_{11}$ (i.e, $Na_2O1.5Fe_2O_3$) was once found in early 1950's [6]. Some researchers reported it as a candidate negative electrode [7] of high capacity in lithium-ion batteries. It becomes necessary to investigate thermodynamic properties of $Na_4Fe_6O_{11}$ in order to understand its role in the Na-Fe-O system. On the other hand, its crystal structure is also of interest because little information was reported for $Na_4Fe_6O_{11}$, either. In the present study, $Na_4Fe_6O_{11}$ was successfully prepared by heating a mixture of $2Na_2CO_3+3Fe_2O_3$ around 1200K. Crystal structure of $Na_4Fe_6O_{11}$ was evaluated by analyzing its X-ray powder diffraction patterns. Vapor pressure measurements over the mixture were done by the Knudsen effusion mass spectrometry (KEMS) in temperature range 913-1023 K. The thermodynamic data of $Na_4Fe_6O_{11}$, such as the standard molar enthalpy of formation, the standard molar Gibbs energy of formation, have been determined. Then, its high temperature stability was discussed too.

To understand the chemical behaviors of sodium ferrates in water vapor and carbon dioxide environments, thermodynamic calculation is essential to obtain equilibrium states. By using the thermodynamic data of the sodium ferrates evaluated in the previous studies, simulation was made in Na-Fe-O-H-C system at high temperatures. Chemical potential diagrams were constructed so that the effects of H_2O and CO_2 were understood. Further experiments have been done to investigate chemical behaviors of Na-Fe oxides in H_2O/CO_2 environments by introducing H_2 and CO_2 into the high temperature mass spectrometer. Experimental results were discussed by comparing with results of theoretic calculations.

2. Investigation of $Na_4Fe_6O_{11}$

Sample manufacture process and the crystal structure determination are given in detail in this section.

2.1 Preparation of $Na_4Fe_6O_{11}$

It is reported that $Na_4Fe_6O_{11}$ (or $Na_2O1.5Fe_2O_3$) could be produced by heating sodium carbonate Na_2CO_3 with ferric oxide Fe_2O_3 (2:3). In 1959, Robert Collongues et Jeanine Thery[6] (a laboratory in France) once obtained $Na_4Fe_6O_{11}$ in this way at 820°C but the data quality of their X-ray diffraction pattern was too poor to carry out further structure analysis. In 1961, Watanabe and Fukase analyzed crystal structures of

$Na_xFe_{2-x}O_{3-x}$ ($0.7<x<1.3$). X-ray patterns of $2Na_2O{\cdot}3Fe_2O_3$ (i.e. $Na_4Fe_6O_{11}$) and β–$NaFeO_2$ were given in their report[7]. Recently, Hua et al repeated the manufacture process at 900°C and claimed X-ray powder diffraction of $Na_4Fe_6O_{11}$, too[8]. Unfortunately, there exist some discrepancies among the above results because Hua's pattern seems a little different from that reported by Watanabe and Fukase.

In this study, same process was employed in which $2Na_2CO_3+3Fe_2O_3$ was utilized as the stating materials. Fine powders of Na_2CO_3 (99.999%, RARE METALLIC Co., Ltd.) and Fe_2O_3 (99.999%, SOEKAWA CHEMICALS) as shown in Fig. 2 were mixed and pressed into plate with molar ration of 2:3 in Ar atmosphere. Then the sample was sintered around 900°C for about 24 hours. A black colored phase (identified as $Na_4Fe_6O_{11}$ later) was produced though a trace amount of the starting materials Na_2CO_3 in white and Fe_2O_3 in red could also be observed.

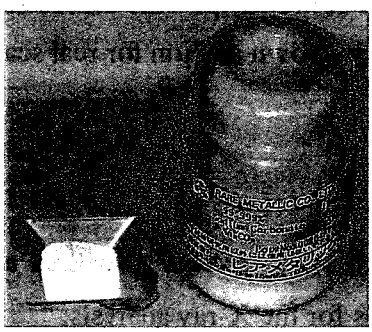

(a) Na_2CO_3, white

(b) Fe_2O_3, red

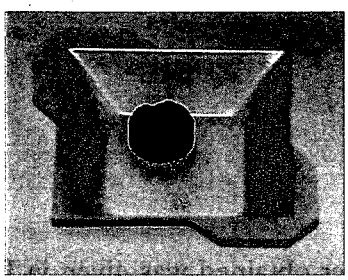

(c) Pellet before sintering, red

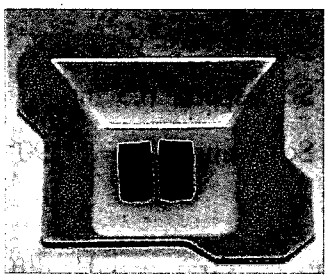

(d) Pellet after sintering, black

Fig. 2 : Source materials and the sintering sample

A photograph (taken by an optical lens with a magnifying power of 1000×) shows that the X-ray analysis sample has an average grain size of about 2 μm (Fig. 3).

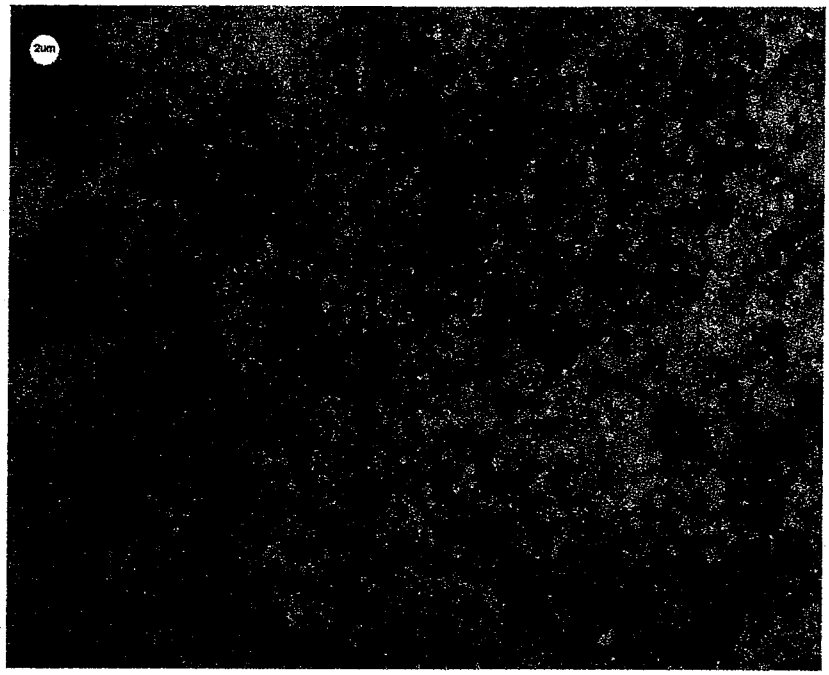

Fig. 3: Photograph of $Na_4Fe_6O_{11}$ sample for X-ray powder diffraction
(Note: the circle in the upper left corner is shown as 2μm for real scale)

2.2 X-ray powder diffraction of $Na_4Fe_6O_{11}$

The prepared sample as described in the last section was than analyzed by X-ray powder diffraction. Here are the conditions for the X-ray analysis:

Radiation source: Cu, $\lambda_{K\alpha 1}$ =1.54050 Å

Sample size: ϕ =7 mm, thickness 0.5-3.0 mm

Scan speed: 0.5°/min

Scan range: 2θ = 10-90°

A typical X-ray powder diffraction patter obtained was given in Fig. 4. For comparison, those patterns given by Watanabe and Fukase, Hua et al. were also shown in Fig. 5-7.

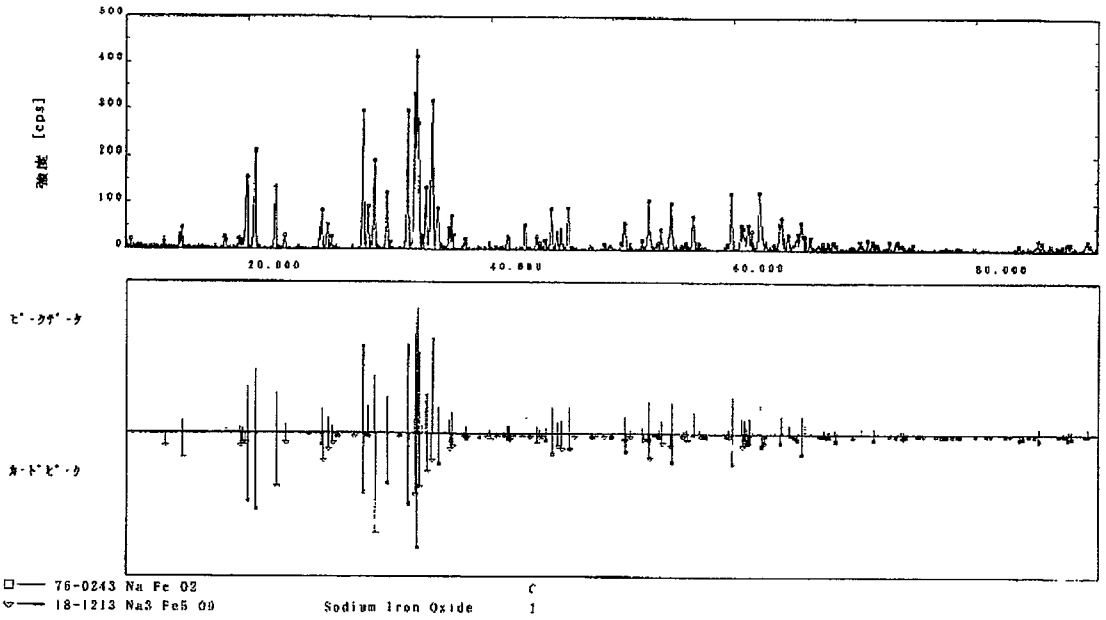

Fig. 4: X-ray diffraction pattern of the $Na_4Fe_6O_{11}$ sample scanned at room temperature

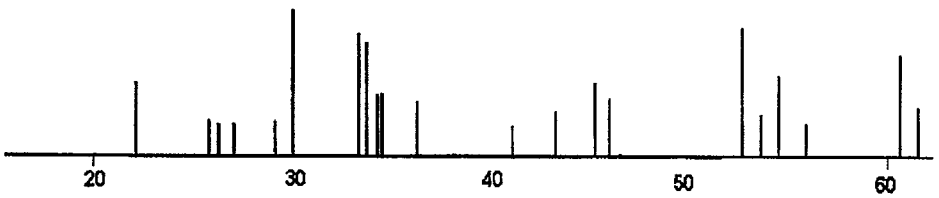

Fig. 5: X-ray diffraction pattern of $Na_4Fe_6O_{11}$ reported by Watanabe and Fukase

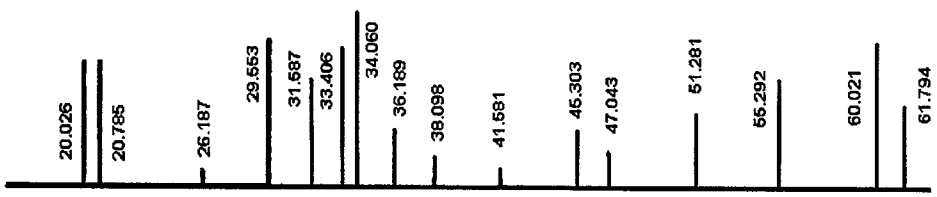

Fig. 6: X-ray diffraction pattern of β–$NaFeO_2$ reported by Watanabe and Fukase

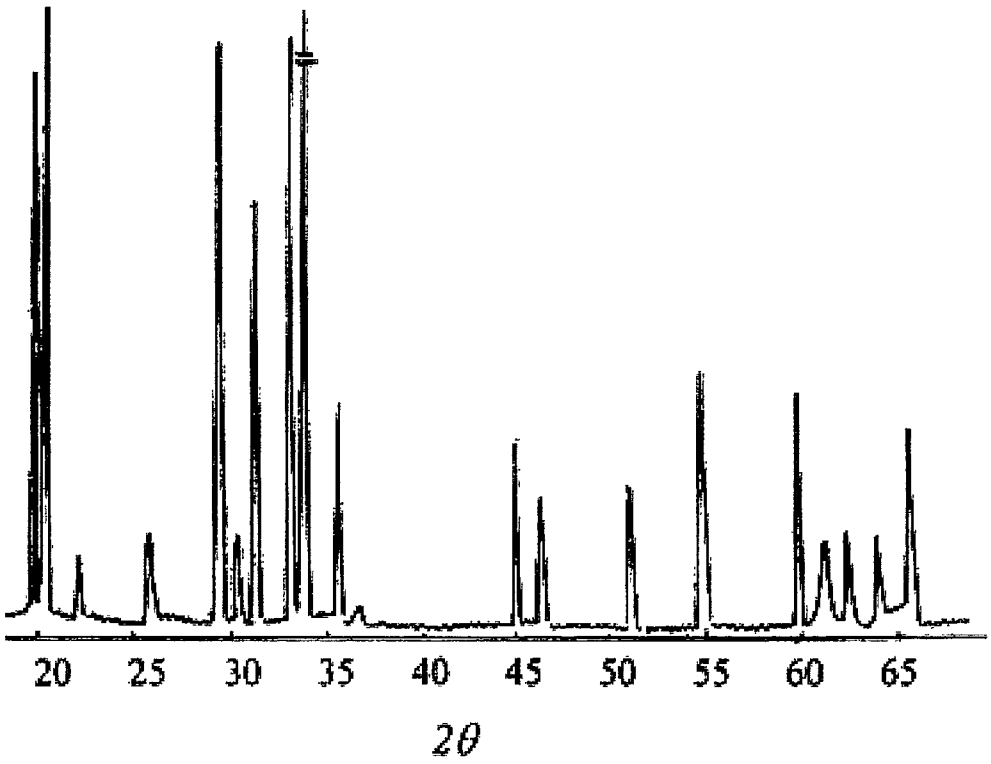

Fig. 7: X-ray diffraction pattern of $Na_2O \cdot 1.5Fe_2O_3$ obtained by Hua et al.

Generally, it is clear that the spectrum of the present sample is quite consistent to those given by Hua et al. Some discrepancy in peak intensities might be attributed to difference in some physical features of the testing powders, such as surface condition, grain size distribution etc...

We also noticed that the X-ray pattern scanned at room temperature after the high temperature experiments looks like a mixture of $Na_3Fe_5O_9$+β–$NaFeO_2$. Watanabe and Fukase's result was a little different from the present result as well as that reported by Hua et al. The possible reasons for the discrepancies in X-ray diffraction patterns will be discussed later in section 3.3 from thermodynamic point of view.

2.3 Structural analysis of $Na_4Fe_6O_{11}$

A powder-indexing program TREOR90 was employed to search for possible geometry for $Na_4Fe_6O_{11}$. Werner described the principle in detail[9]. All the observed 21 main peaks were employed for the fitting program. A satisfied solution found by TREOR90. Index and strength calculation results for each line were given in Table 1, too. It suggests that the triclinic geometry might be a possible symmetry for structure of

$Na_4Fe_6O_{11}$ compound.

Table 1: Indexed powder X-ray diffraction data of $Na_4Fe_6O_{11}$ of the monoclinic system with the cell parameters a=13.4622Å, b=5.3886Å, c=9.1317Å, α=90°, β=96.35°, γ=90.0°.

(h	k	l)	2θ-Obs	2θ-Calc	$\Delta(2\theta)$	d-Obs, Å
3	0	0		19.892		
-1	1	1		19.905		
-1	0	2	19.950	19.938	.000037	4.4470
1	1	1	20.620	20.621	-.000002	4.3040
4	0	1		29.439		
0	0	3	29.510	29.503	.000030	3.0245
-1	0	3		29.520		
3	0	2		29.572		
2	1	2	29.992	29.965	.000120	2.9770
-4	0	2		31.395		
4	1	0	31.465	31.454	.000053	2.8409
0	2	0	33.220	33.225	-.000025	2.6947
-3	0	3		33.888		
4	1	1		33.901		
1	2	0		33.912		
0	1	3		33.957		
-1	1	3	33.970	33.971	-.000006	2.6369
3	1	2		34.018		
1	1	3		35.279		
-2	1	3	35.310	35.322	-.000060	2.5399
-4	1	2	35.700	35.637	.000323	2.5130
-3	2	2	42.920	42.929	-.000052	2.1055
4	2	1		44.976		
0	2	3		45.020		
-1	2	3	45.030	45.032	-.000013	2.0116
3	2	2		45.069		
-6	1	2	46.430	46.465	-.000224	1.9542
3	2	3	51.110	51.117	-.000047	1.7857
8	0	0	54.850	54.849	.000005	1.6724
3	0	5	56.770	56.790	-.000145	1.6203
4	3	1		59.798		
0	3	3		59.834		
-1	3	3	59.850	59.843	.000050	1.5441
3	3	2		59.873		
-7	2	2	61.010	61.031	-.000164	1.5175
-7	1	4	62.330	62.334	-.000033	1.4885
-3	3	3		62.464		
1	0	6	62.490	62.502	-.000092	1.4851
-2	1	6	63.920	63.904	.000127	1.4552
8	2	0	65.680	65.654	.000210	1.4204

The unit cell of $Na_4Fe_6O_{11}$ can be expressed as the following.

Table 2: Unit parameters of $Na_4Fe_6O_{11}$

Vector, Å		Angle	
a	13.4622±0.0037	α	90.00±0.00°
b	5.3886±0.0031	β	96.35±0.03°
c	9.1317±0.002491	γ	90.00±0.00°
Unit cell volume = 658.37 $Å^3$			

It should be noted that an early study by the French [7] derived a tetragonal structure, $a=b=7.2$ Å, $c=18.2$ Å. The space group and atom configurations are still hard to determine at the moment. The present study, however, gave a tentative result for future study in detail.

2.3 Vapor pressure measurement by KEMS

Fine powders of Na_2CO_3 (RARE METALLIC Co., Ltd., 99.999%) and Fe_2O_3 (SOEKAWA CHEMICALS, 99.999%) were mixed and pressed into plate with molar ration of 2:3 in Ar atmosphere. Then the sample was installed in the Knudsen cell made of Pt. The detail of the high temperature mass spectrometer can be found in our previous paper [4]. The orifice used in the experiment was in diameter of 1mm.

Baking process was carried out around 827K for over 24 hours until the absorption gas impurities such as water vapor and carbon dioxide in the sample were deduced to the background level. The vapor pressure measurements were conducted from about 870-1010K. CO_2 was found as the main vapor species during our experimental measurement. No evidence of sodium or sodium hydroxide was detected in the experiments. CO could be identified but its intensity was observed close to the background level. So, the electron impact energy was set to be 20 eV to obtain large ion intensity. Pressure calibration was made by using pure silver as the standard reference. So, the pressure of CO_2 is calculated as the following equations:

$$p(CO_2) = K^*[I(CO_2^+)^*T]/\sigma(CO_2) \quad \text{.....(1)}$$

$$K = p(Ag)^* \ \sigma(Ag)/[I(Ag+)^*T] \quad \text{.....(2)}$$

where, p is the absolute vapor pressure, I is the ion intensity measured by the mass spectrometer, and σ is the electron impact ionization cross-section. The electron ionization cross-sections of CO_2 and Ag at 20 eV were taken from literatures, i.e., $\sigma(CO_2)/M^2 = 0.508 \times 10^{-20}$ [9] and $\sigma(Ag)/M^2 = 4.50 \times 10^{-20}$ [10].

After the mass spectrometric measurement, a black colored product $Na_4Fe_6O_{11}$ was found together with the starting materials Na_2CO_3 in white and Fe_2O_3 in red. The sample was analyzed by X-ray powder diffraction. Peaks of $Na_4Fe_6O_{11}$ were identified. Since no evidence of other sodium-containing compounds was found, decomposition of Na_2CO_3 into Na_2O or formation of other possible sodium-iron complex oxides such as $NaFeO_2$ or $Na_3Fe_5O_9$ etc... can be ruled out.

At the beginning of reaction (within the first 20 hours of sintering), only Na_2CO_3 and Fe_2O_3 can be easily identified by X-ray powder diffraction as shown in Fig. 3. A few peaks of product $Na_4Fe_6O_{11}$ could also be found. After three days measurement around 1000K, the X-ray powder diffraction result clearly shows $Na_4Fe_6O_{11}$ became the main compound in the sample as shown in Fig. 8-9.

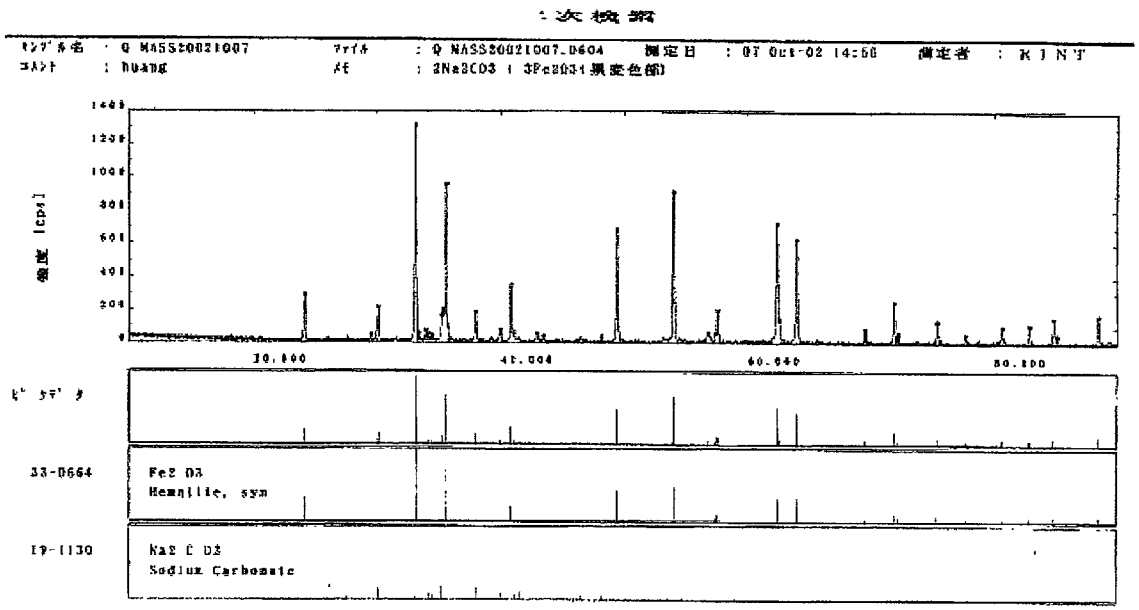

Fig. 8: X-ray pattern of sample in the initial stage of the reaction

So, it is assumed that the following reaction occurred in the Knudsen cell during the mass spectrometric tests.

$$2Na_2CO_3 + 3Fe_2O_3 = Na_4Fe_6O_{11} + 2CO_2(gas) \quad \text{.....(3)}$$

The partial vapor pressures of CO_2 over the mixture of $2Na_2CO_3$ and $3Fe_2O_3$ obtained by the KEMS were given in Table 5 in detail. The first sample of about (50 mg) was measured for about 6 hours around 970 K and the second sample (200 mg) for about 15 hours. Both samples showed very close slope of $\ln P(CO_2)$ against $1000/T$ as shown in Fig. 10 and Table 3. The differences in the absolute pressures for the two samples should be attributed to some minor variation of the sealing performance of the Pt-made Knudsen cell caused by sample handling. The temperature dependences of CO_2 partial pressure can be expressed as the following equation:

$$\ln\{p(CO_2)/\text{Pa}\} = (29.4385 \pm 0.3244) + (-29015.4 \pm 313.55) \times \text{K}/T,$$
$$(913 - 1023\ \text{K}) \quad \text{.....(4)}$$

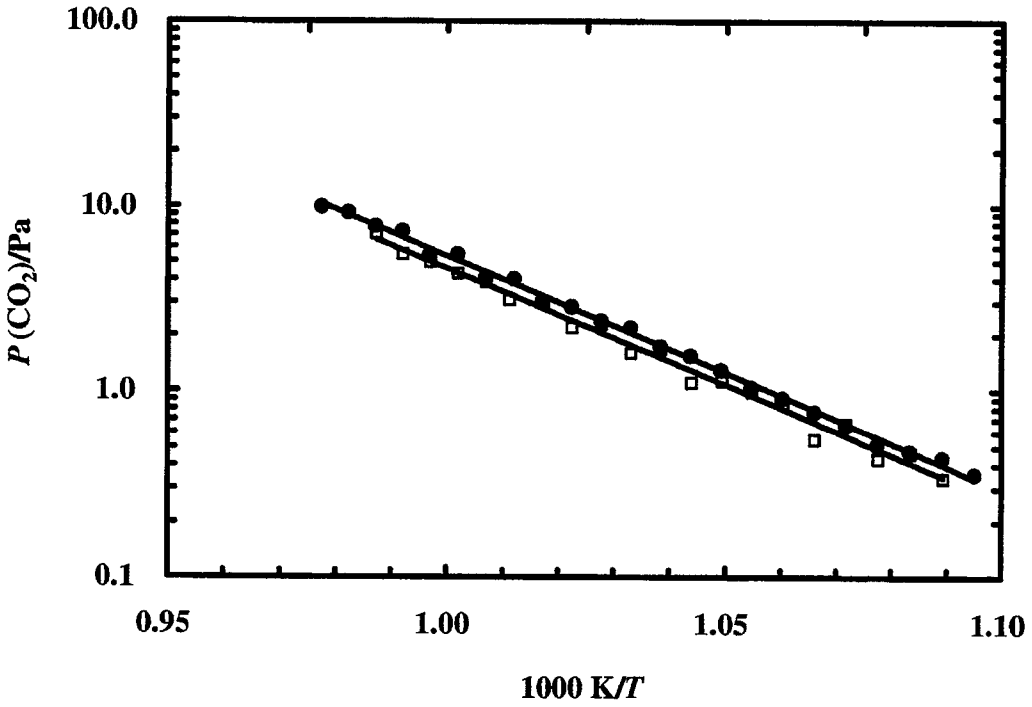

Fig. 9: Pressure-temperature dependence of CO_2 over $2Na_2CO_3$+$3Fe_2O_3$.

□, experiment 1; ●, experiment 2; ——, least squares fitting.

Table 3: Partial CO_2 pressure over the mixture of $2Na_2CO_3+3Fe_2O_3$ obtained by the Knudsen effusion mass spectrometer

	Experiment 1		Experiment 2	
No.	T/K	$p(CO_2)$/Pa	T/K	$p(CO_2)$/Pa
1	923	0.46393	918.15	0.43650
2	933	0.66301	928.15	0.51630
3	943	0.85807	938.15	0.76762
4	953	1.13145	948.15	1.04258
5	963	1.66909	958.15	1.54938
6	973	2.27667	968.15	2.19178
7	983	2.98157	978.15	2.84710
8	993	3.87245	988.15	4.02670
9	1003	4.95450	998.15	5.48782
10	1013	7.11080	1008.15	7.30346
11	1008	5.50332	1018.15	9.21988
12	998	4.32438	913.15	0.36029
13	989	3.08548	923.15	0.47769
14	978	2.20362	933.15	0.65187
15	968	1.59387	943.15	0.91508
16	958	1.11248	953.15	1.29469
17	948	0.98586	963.15	1.74436
18	938	0.55276	973.15	2.39193
19	928	0.43428	983.15	3.05243
20	918	0.34209	993.15	4.11131
21			1003.15	5.45043
22			1013.15	7.79841
23			1023.15	9.92695

2.5 Thermodynamic evaluation of $Na_4Fe_6O_{11}$

Since the temperature-pressure relationship was obtained, further thermodynamic analysis can be done for the reaction $2Na_2CO_3+3Fe_2O_3=Na_4Fe_6O_{11}+2CO_2$(gas). Then, data of $Na_4Fe_6O_{11}$ can be evaluated from the experimental values of vapor pressure of CO_2 as properties of the left substances in the reaction are well known.

The enthalpy change of Eq.(3) at the average temperature of the measurements was calculated as $\Delta_r H°_m(970\ K) = 240.7\pm8\ kJ\cdot mol^{-1}$.

By using thermodynamic data of Na_2CO_3, Fe_2O_3 and CO_2(gas) given in the SGTE database, thermodynamic treatments by the 2nd law and the 3rd law (see Table 4) have been made, respectively. A summary of the evaluation results is listed in Table 5. Standard molar enthalpy of formation of $Na_4Fe_6O_{11}$ at 298.15 K was determined as: $\Delta_f H°_m(Na_4Fe_6O_{11}, 298.15K)\ /J\cdot mol^{-1} = -3569.57 \pm 3.94$.

The standard molar Gibbs energy of formation of $Na_4Fe_6O_{11}$ was derived as:

$$\Delta_f G°_m(Na_4Fe_6O_{11})\ /J\cdot mol^{-1} = (-37033784 \pm 9373.55) + (1197.837 \pm 9.65) \times T/K. \quad \text{... (5)}$$

$\Delta_f G°_m(Na_4Fe_6O_{11}, 298.15\ K)$ could be estimated by employing the following equation:

$$\Delta_f G°_m(Na_4Fe_6O_{11}, 298.15\ K) = \Delta_f H°_m(298.15\ K) - T/K \times \Delta_f S°_m(298.15\ K) \quad \text{... (6)}$$

where, $\Delta_f S°_m(298.15\ K)$ is the standard entropy of formation from its component elements in their standard states. $S°_m(Na_4Fe_6O_{11}, 298.15\ K) = 442\ J\cdot mol^{-1}\cdot K^{-1}$ estimated by Lindemer et al.[1] was utilized for this calculation. Thus, $\Delta_f G°_m(Na_4Fe_6O_{11}, 298.15\ K)$ is recommended as $-3255.3\pm12.4\ kJ\cdot mol^{-1}$. Heat capacity $Cp(Na_4Fe_6O_{11})/ J\cdot mol^{-1}\cdot K^{-1}$ was estimated from its corresponding component binary oxides, i.e.

$$Cp(T) = 523.7+9.678\times10^2\ T-7.386\times10^6/T^2. \quad \text{... (7)}$$

The Gibbs energy function $gef(T)$ was calculated using the following equation:

$$gef_m(T) = [G°_m - H°_m(298.15\ K)]/T$$
$$= -S°_m(T) + [H°_m(T) - H°_m(298.15\ K)]/T \quad \text{... (8)}$$

Table 4: Standard enthalpy of formation of $Na_4Fe_6O_{11}$ by the 3rd law treatment

1st sample		2nd sample	
T(K)	$\Delta_f H°(298)$ J/mol	T(K)	$\Delta_f H°(298)$ J/mol
918.15	-3576525.71	963.15	-3573002.171
928.15	-3574293.748	973.15	-3570763.078
938.15	-3573595.14	983.15	-3569516.042
948.15	-3572292.286	993.15	-3569882.486
958.15	-3571612.36	1003.15	-3566985.317
968.15	-3570599.202	1013.15	-3565409.69
978.15	-3568986.295	923.15	-3575259.361
988.15	-3567968.744	933.15	-3574292.559
998.15	-3566682.996	943.15	-3572660.72
1008.15	-3565215.981	953.15	-3571151.524
1018.15	-3563347.292	963.15	-3570417.821
913.15	-3576924.504	973.15	-3569143.061
923.15	-3575453.136	983.15	-3567575.723
933.15	-3574177.295	993.15	-3565937.564
943.15	-3573097.696	1003.15	-3564176.267
953.15	-3572078.061	1013.15	-3563237.457
963.15	-3570723.547	1008.15	-3563156.765
973.15	-3569489.046	998.15	-3564966.666
983.15	-3567741.405	989.15	-3565718.658
993.15	-3566365.76	978.15	-3567177.649
1003.15	-3564866.268	968.15	-3568373.179
1013.15	-3563911.721	958.15	-3569321.372
1023.15	-3562089.621	948.15	-3571910.291
		938.15	-3571371.528
		928.15	-3573135.229
		918.15	-3574910.759

Table 5: Vapor pressure measurement results for $2Na_2CO_3+3Fe_2O_3=Na_4Fe_6O_{11}+2CO_2$ and corresponding thermodynamic evaluations

	Experiment 1	Experiment 2
$\ln\{p(CO_2)/Pa\}$ $= A + B \times K/T$ (913 - 1023 K)	*A*	*B*
	28.8976±0.9536	29.4385±0.3244
	B	*B*
	-28880.5±923.19	-29015.4±313.55
$\Delta_r H°_m<T>/K$ /kJ·mol^{-1} *	240.1±7.7	241.2±2.6
By the 2nd law treatment $\Delta_f H°_m(Na_4Fe_6O_{11}, 298.15 K)$ /J·mol^{-1}	-3641.2±77.9	-3656.2±86.2
	Averaged: -3648.7 ± 87	
By the 3rd law treatment $\Delta_f H°_m(Na_4Fe_6O_{11}, 298.15 K)$ /J·mol^{-1}	-3569.26±3.39	-3569.91±4.37
	Averaged: -3569.54 ± 3.95	
$\Delta_f G°_m(Na_4Fe_6O_{11})$ /J·mol^{-1} $= C + D \times T/K$ (913 - 1023 K)	*C*	*C*
	-37033784±9373.55	-3716839±2274.55
	D	*D*
	1197.837±9.65	-1200.16±2.35
$\Delta_f G°_m(Na_4Fe_6O_{11}, 298.15 K)$ /kJ·mol^{-1}	-3254.90±12.3	-3255.60±12.4
	Recommended: -3255.3±12.4	

*: <*T*> is the average temperature of the measurement.

We also noticed that $\Delta_f H°_m(Na_4Fe_6O_{11}, 298.15K)$ of $Na_4Fe_6O_{11}$ obtained by the 2nd law method in the present study (-3648.7 kJ·mol^{-1}·K^{-1}) is quite close to the -3665 kJ·mol^{-1}·K^{-1} derived from the 2nd law by Lindemer[1]. However, his estimation was mainly based on Knight and Philips' early experiment and could only provided a rough results. According to the more precise measurements in the present study, more accurate value evaluated by the 3rd law treatment is recommended, i.e., $\Delta_f H°_m(Na_4Fe_6O_{11}, 298.15K)$= -3569.54 kJ·mol^{-1}·K^{-1}.

Thus, the thermodynamic table for $Na_4Fe_6O_{11}$ is built up in Table 6.

Table 6: The standard molar thermodynamic functions of $Na_4Fe_6O_{11}$

T K	$C_{p,m}(T)$ $J \cdot mol^{-1} \cdot K^{-1}$	$S°_m(T)$ $J \cdot mol^{-1} \cdot K^{-1}$	$H°_m - H°_m($298.15 K$)$ $kJ \cdot mol^{-1}$	$gef(T)$ $J \cdot mol^{-1} \cdot K^{-1}$	$\Delta_f H°_m(T/K)$ $kJ \cdot mol^{-1}$	$\Delta_f G°_m(T/K)$ $kJ \cdot mol^{-1}$
298.15	469.467	442.000	0.000	-442.000	-3569.540	-3255.260
300	470.667	444.908	0.870	-442.009	-3569.456	-3253.310
371	505.944	548.821	35.646	-452.740	-3565.687	-3178.885
371	Na: melting point 2.60					
371	505.944	548.821	35.646	-452.740	-3576.079	-3178.885
400	516.249	587.293	50.472	-461.113	-3574.430	-3147.898
500	542.546	705.522	103.504	-498.514	-3567.800	-3042.002
600	561.251	806.168	158.735	-541.610	-3560.508	-2937.519
700	576.373	893.853	215.637	-585.800	-3553.321	-2834.258
800	589.583	971.695	273.947	-629.262	-3546.903	-2731.982
900	601.683	1041.845	333.517	-671.270	-3541.896	-2630.432
1000	613.094	1105.834	394.261	-711.573	-3538.940	-2529.336
1042	617.742	1131.153	420.108	-727.978	-3538.464	-2486.944
1042	Fe: melting point 0.75					
1042	617.742	1131.153	420.108	-727.978	-3542.964	-2486.944
1100	624.054	1164.785	456.121	-750.130	-3542.052	-2428.176
1170	631.584	1203.752	500.345	-776.267	-3538.319	-2356.950
1170	[Na:] 97.25					
1170	631.584	1203.752	500.345	-776.267	-3927.303	-2356.950
1184	633.019	1211.035	508.919	-781.204	-3925.889	-2338.765
1184	[Fe:tp] 0.90					
1184	633.019	1211.035	508.919	-781.204	-3931.289	-2338.765
1200	634.707	1219.543	519.061	-786.992	-3928.824	-2317.261
1300	645.144	1270.760	583.055	-822.256	-3913.194	-2183.593
1400	655.424	1318.948	648.085	-856.030	-3897.183	-2051.143
1500	665.587	1364.514	714.136	-888.424	-3880.795	-1919.851

2.6 Chemical stability of $Na_4Fe_6O_{11}$ at high temperatures

It should be noted that $NaFeO_2$ and $Na_3Fe_5O_9$ were often observed in the products if the synthesis process of $Na_4Fe_6O_{11}$ was carried out between 1030K and 1270K. The XRD patterns were of two samples prepared at 1000K and 1173K were given in Fig. 10 and Fig. 11, respectively. As shown in Fig. 10, the main products at 1000K seemed $NaFeO_2$ and Fe_2O_3, while $Na_3Fe_5O_9$ and $NaFeO_2$ were the main phases at 1173K. Both examples indicated an important fact that $Na_4Fe_6O_{11}$ decomposed in these temperature conditions. According to our early thermodynamic studies, $Na_3Fe_5O_9$ is stable over 1030K. When temperature is lower than 1030K, the stable product should be $NaFeO_2$ and Fe_2O_3. This is in good consistent with the above experimental results.

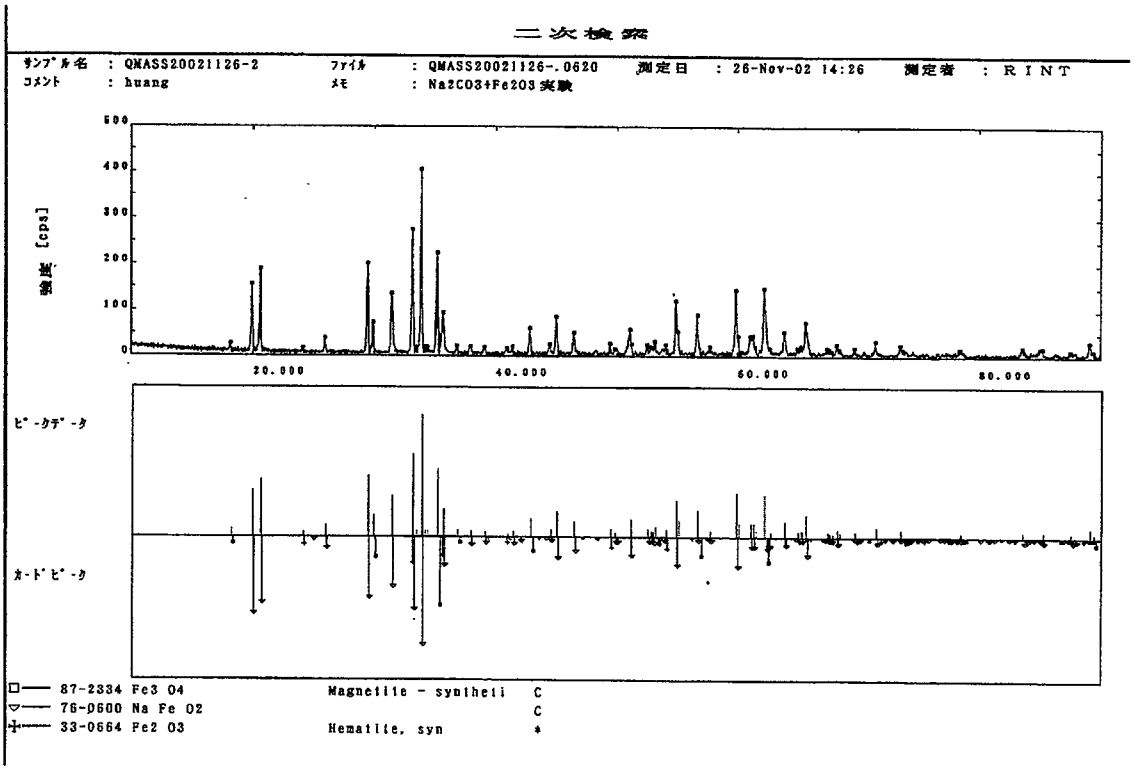

Fig. 10: X-ray pattern of sample after long time measurement at 1000K

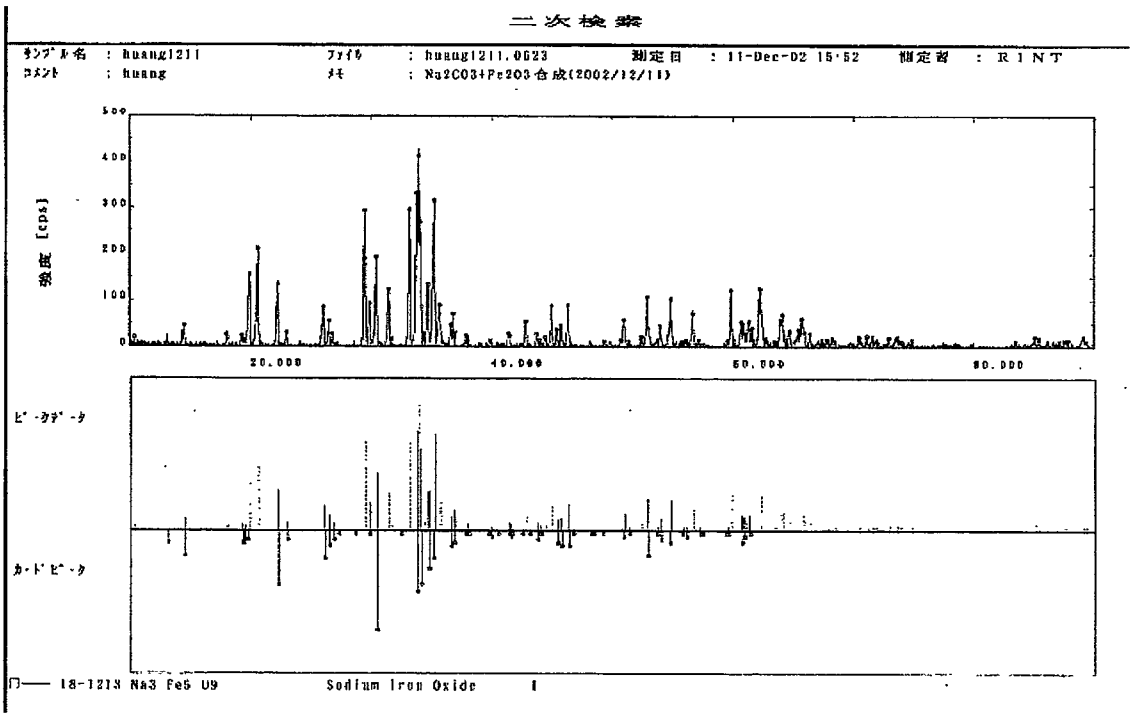

Fig. 11: X-ray pattern of sample after long time measurement at 1173K

By using Thermo-Calc code, equilibrium calculations were made and some predominant phase diagrams were made from 1000-1300 K. It shows that there is no $Na_4Fe_6O_{11}$ from room temperature to 1270K. It suggests that $Na_4Fe_6O_{11}$ should be likely to decompose into other forms of Na-Fe oxides at lower temperature range.

For instance,

$Na_4Fe_6O_{11} \rightarrow Na_3Fe_5O_9 + NaFeO_2$ when $1030<T<1270$K (Fig. 12-13);

$Na_4Fe_6O_{11} \rightarrow NaFeO_2 + Fe_2O_3$ when $T<1030$K (Fig.14).

A ternary phase diagram of Na-Fe-O at 1100K was given in Fig. 15.

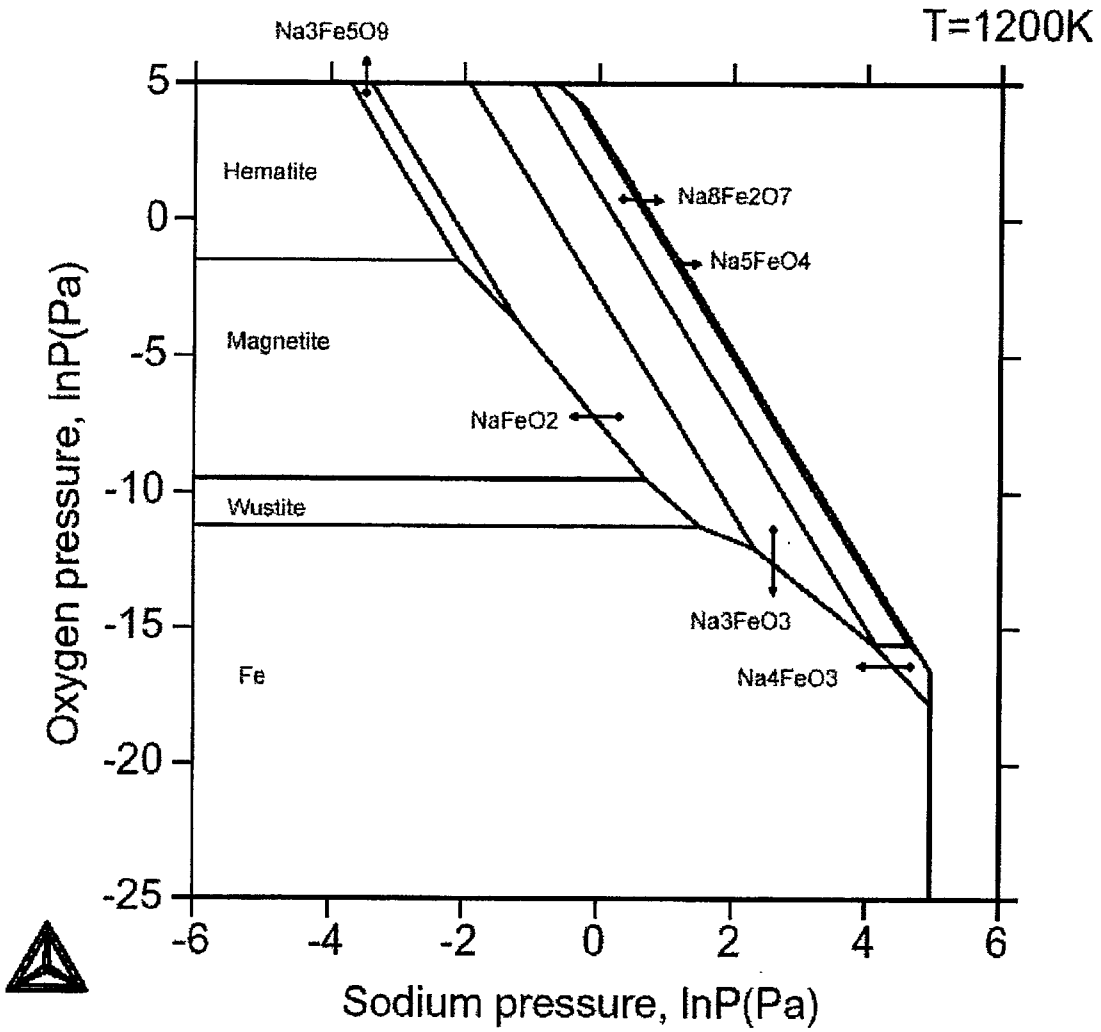

Fig. 12: Predominance diagram of Na-Fe-O at 1200 K

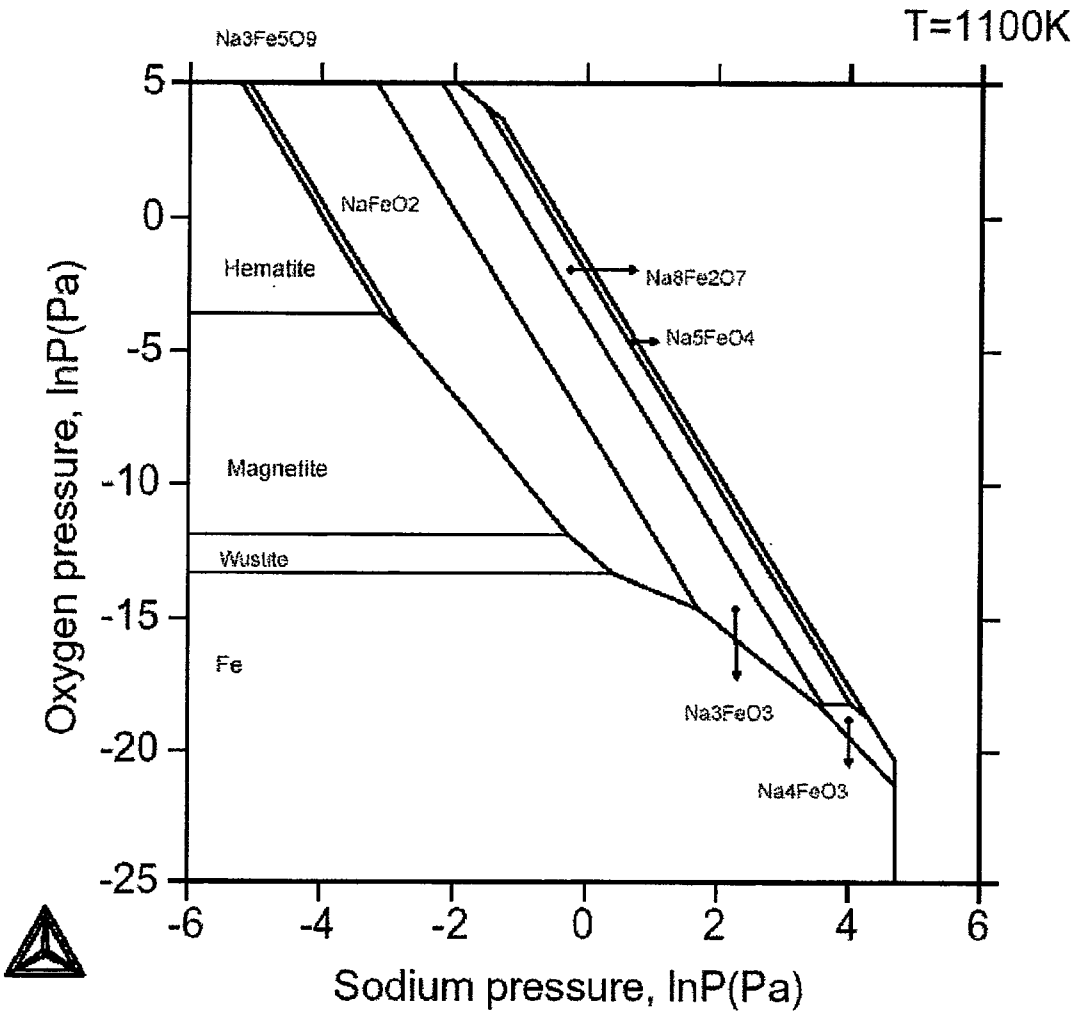

Fig. 13: Predominance diagram of Na-Fe-O at 1100 K

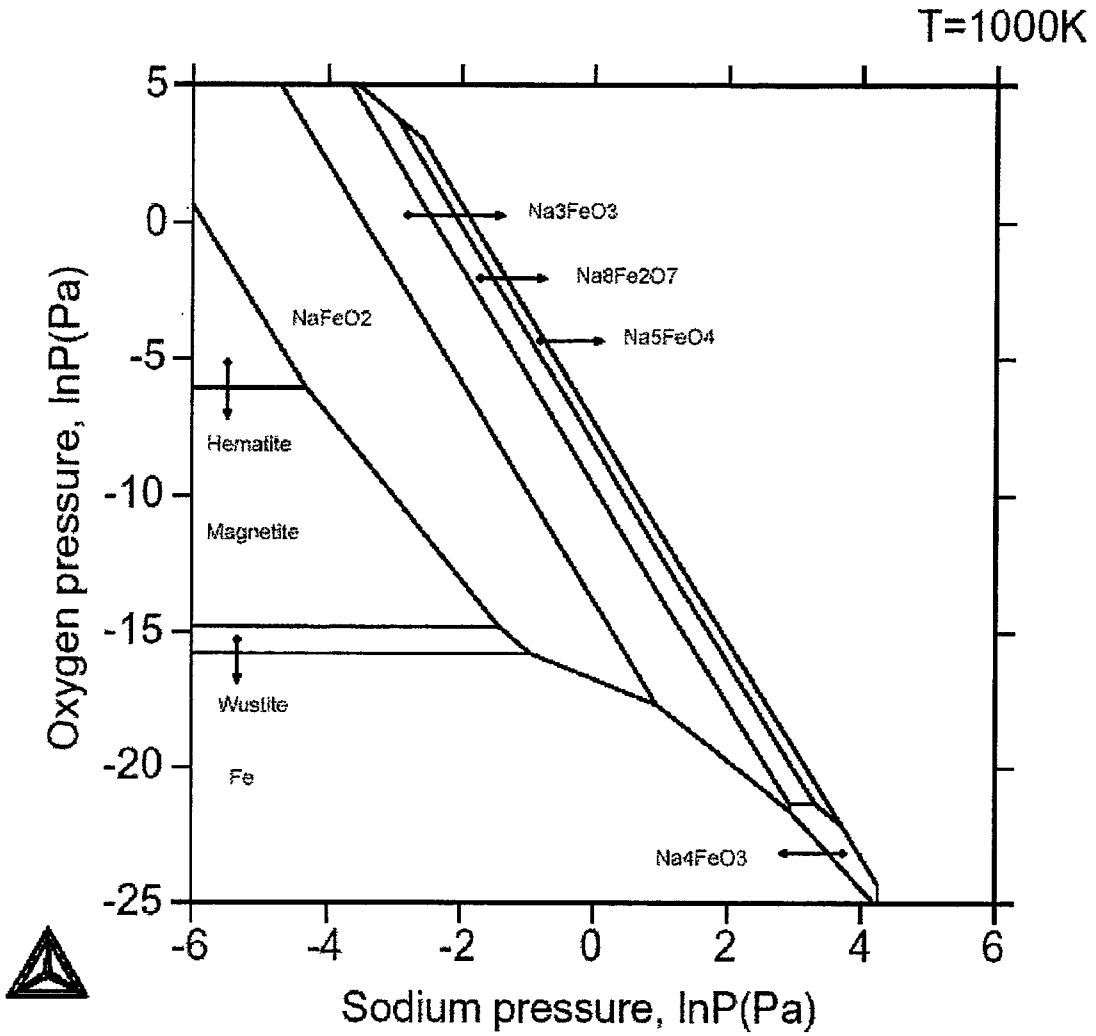

Fig. 14: Predominance diagram of Na-Fe-O at 1000 K

Therefore, $Na_4Fe_6O_{11}$ should be considered as a metastable phase if it appeared at relatively low temperatures. This may be the main reason why $NaFeO_2$ and $Na_3Fe_5O_9$ were easily found together with $Na_4Fe_6O_{11}$ in X-ray powder diffraction analysis. Taking this factor into account, the little difference of X-ray diffraction patterns of $Na_4Fe_6O_{11}$ between Watanabe's and Hua's would be reasonable.

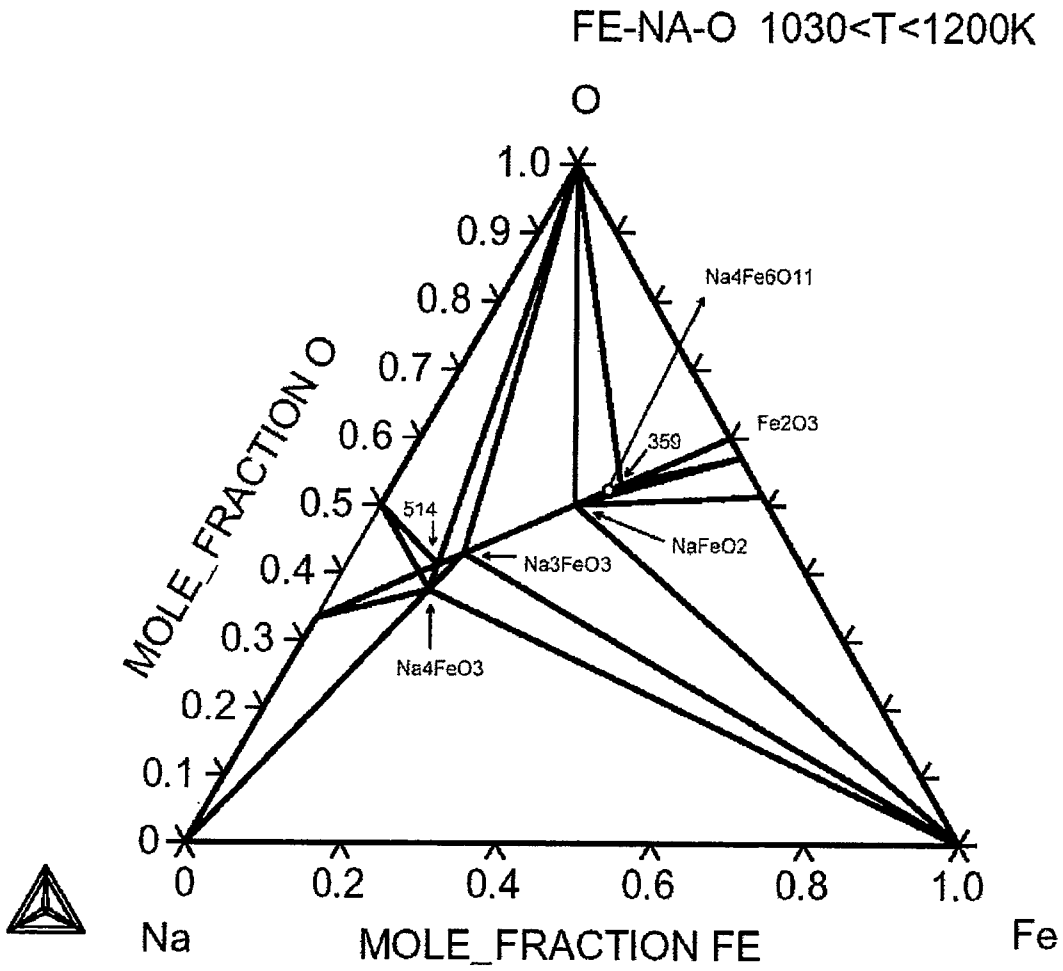

Fig. 15 : Ternary phase diagram of Na-Fe-O at 1100 K

As for the possible temperatures in case of sodium-leak accident in FBR, many researches have been done. For example, the highest temperature in Na-H_2O reaction was found around 1300-1500K. From the thermodynamic analysis in this report, it may not be strange in theory if $Na_4Fe_6O_{11}$ would have been formed. However, the probability would be very low because the highest temperature was only temporally reached while the average temperature in the reaction zone would be only around several hundreds degrees.

3. Thermodynamic analyses of Na-Fe-O-H-C system

Theoretic calculations of sodium ferrates in H_2O/CO_2 environments were carried out. Experiments by gas-inlet KEMS have been done to investigate influence of water vapor and carbon dioxides on chemical behaviors of sodium ferrates.

3.1 Equilibrium calculations for the chemical potential diagrams

The thermodynamic data of $NaFeO_2$, Na_3FeO_3, Na_5FeO_4, $Na_8Fe_2O_7$, $Na_3Fe_5O_9$ as well as Na_4FeO_3 have been given in the previous studies. Analyses of $Na_4Fe_6O_{11}$ were described in section 2. Those of $Na_3Fe_5O_9$ need to be evaluated by using some data reported in literatures.

Kale and Srikanth[12] obtained the Gibbs energy of formation of $Na_3Fe_5O_9$ by using solid-state electrochemical cells where $\Delta G°(Na_3Fe_5O_9)$ from solid Na_2O and α–Fe_2O_3 was derived as the following.

$$\Delta G°(Na_3Fe_5O_9)\ (J/mol) = -307956 + 64.64T \qquad (1025\text{-}1137K) \ \ldots\ldots\ldots (9)$$

They further conclude that $Na_3Fe_5O_9$ should decompose to $Na_3Fe_5O_9$ and Fe_2O_3 at 1029K. The Gibbs energy change for the following reaction is determined as

$$\Delta_r G°(J/mol) = 40917 - 39.775T \quad (3/2Na_3Fe_5O_9 + Fe_2O_3 .\ \ Na_3Fe_5O_9) \qquad \ldots\ldots\ldots (10)$$

So, the standard Gibbs energy of formation of $Na_3Fe_5O_9$ was estimated as $\Delta_f G°(Na_3Fe_5O_9)$ = –2646.0 kJ/mol while the standard enthalpy of formation of $Na_3Fe_5O_9$ was evaluated as $\Delta_f H°(Na_3Fe_5O_9)$ = –2904.4 kJ/mol. A thermodynamic table of $Na_3Fe_5O_9$ (Table 7) was built up by using the entropy $S°(298)$= 346 J/molK estimated by Lindemer, heat capacity $Cp(T)$= $422.93+7.819\times10^{2}\ T-5.907\times10^{6}/T^{2}$ estimated from its corresponding simple oxides as given by MALT2.

Thus, equilibrium calculation of sodium ferrates in water vapor and carbon dioxide environments can be done by using thermo-Calc code. All the thermodynamic data in the Na-Fe-O-H-C system were periodically taken from the SGTE database supplied together with Thermo-Calc. Those of Na-Fe oxides were mainly based on our previous works.

Table 7: Thermodynamic table of $Na_3Fe_5O_9$

T	*Cp*	*S*°	*H*°-*H*°(298)	*gef*	$\Delta_f H°$	$\Delta_f G°$
K	J/K·mol	J/K·mol	kJ/mol	J/K·mol	kJ/mol	kJ/mol
298.15	379.792	346	0	-346	-2904.4	-2646
300	380.754	348.352	0.704	-346.007	-2904.33	-2644.4
371	409.022	432.384	28.826	-354.686	-2901.17	-2583.22
371	[Na:mp] 2.6					
371	409.022	432.384	28.826	-354.686	-2908.97	-2583.22
400	417.287	463.483	40.811	-361.457	-2907.58	-2557.81
500	438.397	559.031	83.669	-391.694	-2902.1	-2470.98
600	453.436	640.35	128.293	-426.528	-2896.15	-2385.31
700	465.608	711.187	174.262	-462.241	-2890.36	-2300.64
800	476.252	774.068	221.365	-497.362	-2885.25	-2216.76
900	486.008	830.732	269.483	-531.306	-2881.35	-2133.44
1000	495.213	882.418	318.548	-563.87	-2879.19	-2050.48
1042	498.964	902.869	339.426	-577.125	-2878.93	-2015.68
1042	[Fe:mtp] 0.75					
1042	498.964	902.869	339.426	-577.125	-2882.68	-2015.68
1100	504.057	930.034	368.514	-595.022	-2882.12	-1967.43
1170.44	510.135	961.508	404.234	-616.139	-2879.25	-1908.93
1170.44	[Na:] 97.25					
1170.44	510.135	961.508	404.234	-616.139	-3170.98	-1908.93
1184	511.293	967.391	411.16	-620.128	-3169.89	-1894.32
1184	[Fe:tp] 0.9					
1184	511.293	967.391	411.16	-620.128	-3174.39	-1894.32
1200	512.656	974.263	419.351	-624.804	-3172.44	-1877.03
1300	521.082	1015.631	471.039	-653.293	-3160.06	-1769.58
1400	529.382	1054.552	523.563	-680.578	-3147.4	-1663.1
1500	537.59	1091.356	576.913	-706.747	-3134.44	-1557.53

Chemical potential diagram plotted as functions of oxygen pressure and sodium pressure were constructed at high temperatures. According to the equilibrium calculations, CO_2 may react with Na-Fe oxides and Na_2CO_3 may be formed when partial vapor pressure of CO_2 is high enough. Take 800K as an example, if the $P_{CO2}=10^{-3}$ Pa, the main stable compounds in the system would be $NaFeO_2$ and Na_2CO_3 as shown in Fig. 16.

Other Na-Fe oxides such as Na_5FeO_4, $Na_8Fe_2O_7$ as well as Na_3FeO_3 tend to be no longer stable because of the presence of CO_2. Possible reactions would be like,

$$CO_2 + Na_5FeO_4 \rightarrow Na_2CO_3 + Na_3FeO_3 \quad \ldots\ldots\ldots (11)$$

$$CO_2 + Na_3FeO_3 \rightarrow Na_2CO_3 + NaFeO_2 \quad \ldots\ldots\ldots (12)$$

.....and so on.

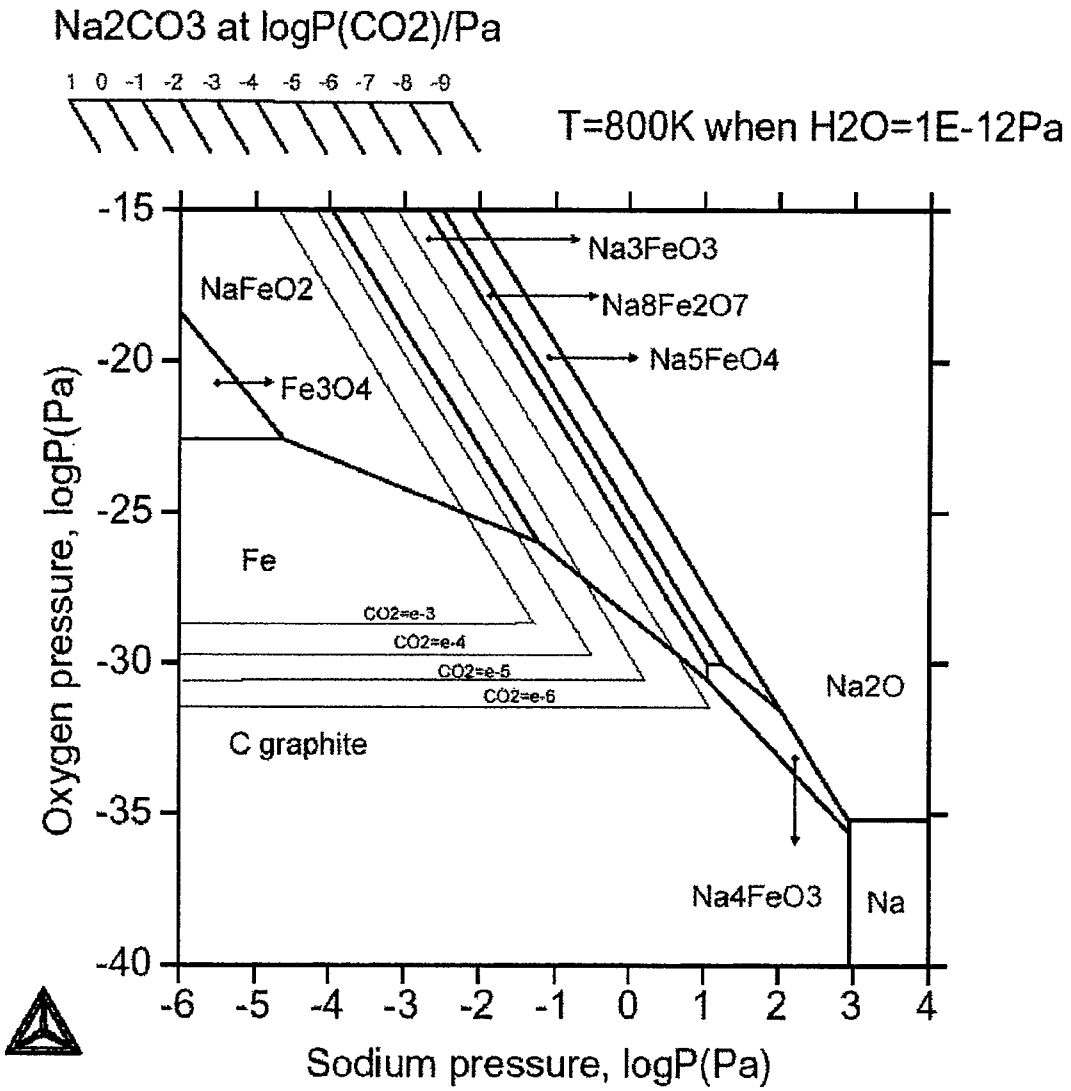

Fig. 16: Chemical potential diagram of Na-Fe-O-H-C system at 800K when water vapor pressure is fixed at 1E-12 Pascal.

Similar calculations were also done to investigate effect of water vapor. The formation of NaOH+$NaFeO_2$ requires that water vapor pressure reaches as high as about 1 Pa level as shown in Fig. 17.

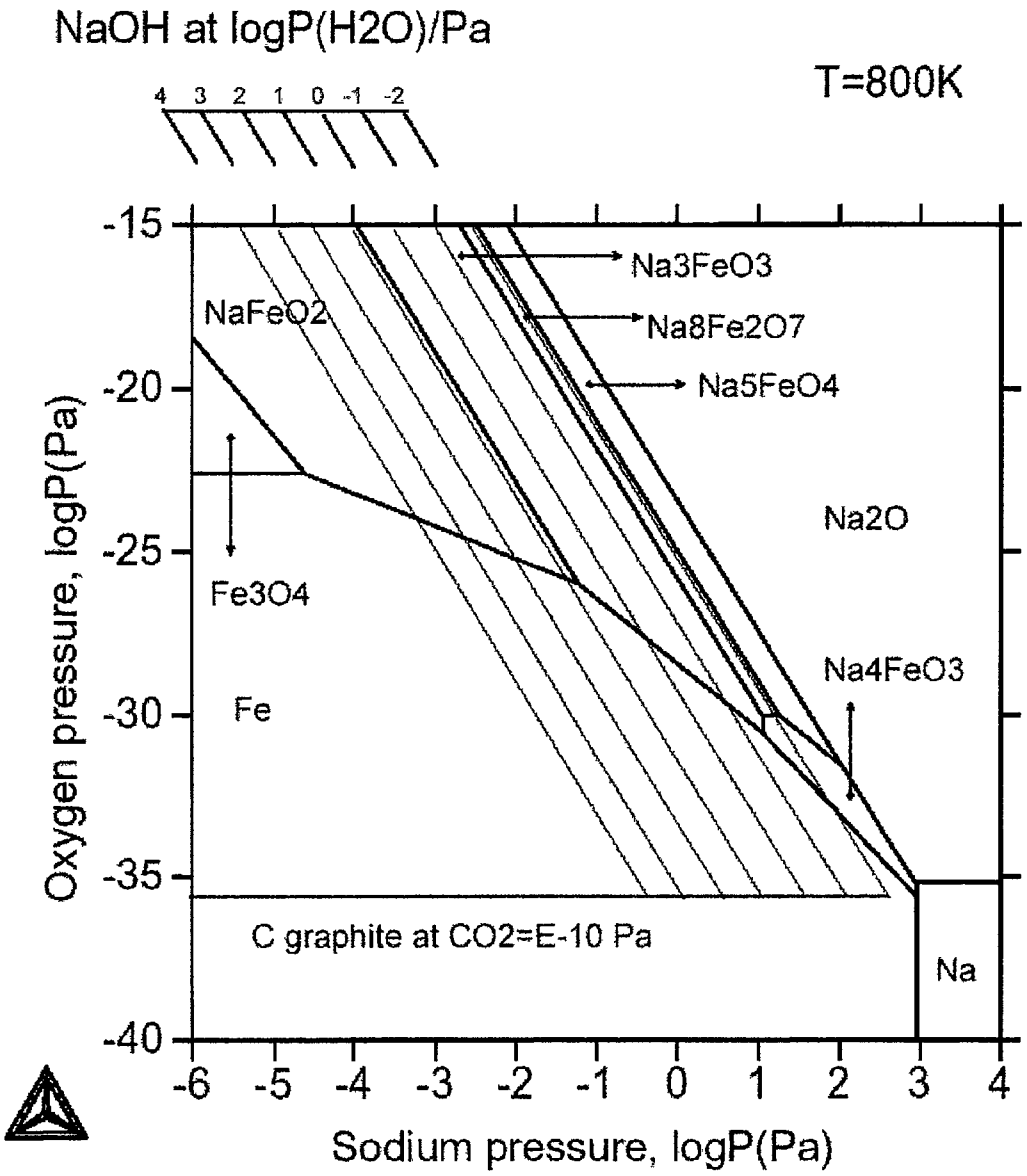

Fig. 17: Chemical potential diagram of Na-Fe-O-H-C system at 800K when carbon dioxide pressure is fixed at 1E-10 Pa.

3.2 The gas-inlet KEMS equipment

To test the influence of water vapor and carbon dioxide on chemical behaviors of sodium ferrates, a gas-inlet high temperature mass spectrometer was built. As shown in Fig. 18-19, two fine tubes were connected to the Knudsen cell (KC) so that gases like H_2 and CO_2 could be introduced into the cell to react with Na-Fe oxides samples. Then, the partial vapor pressures of main vapor species in the system could be measured by the KEMS.

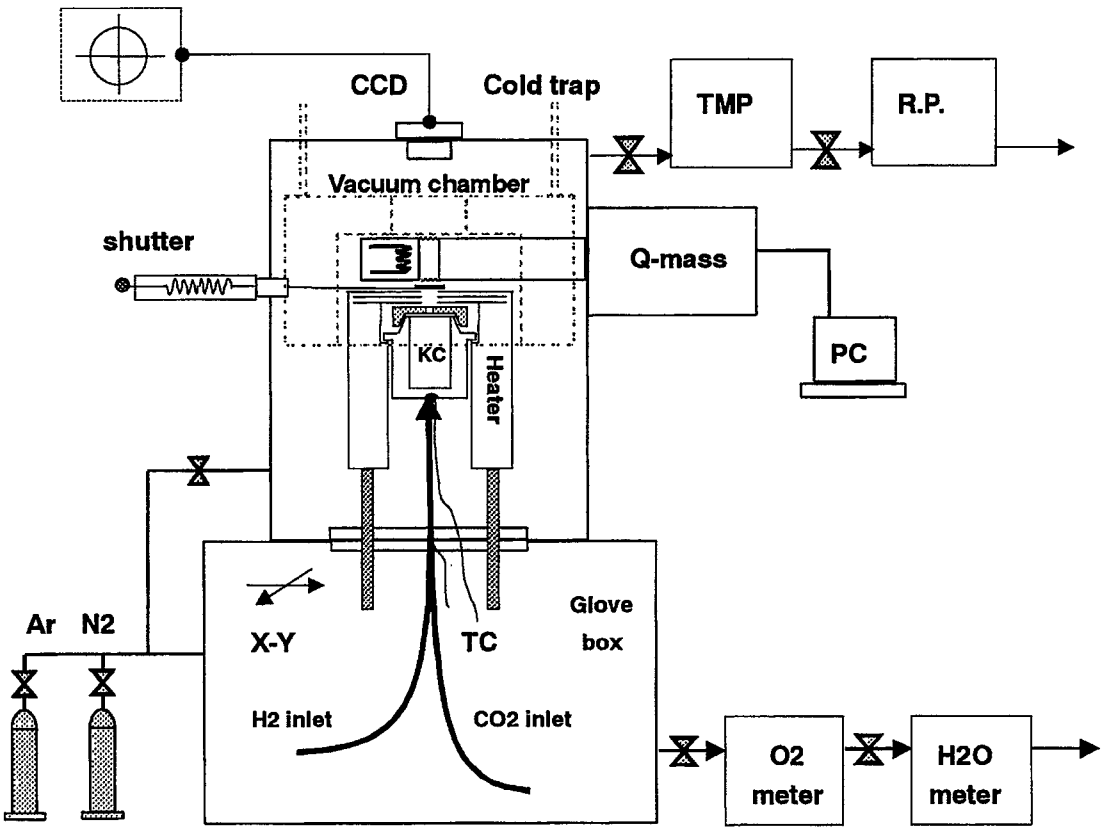

Fig. 18 : Schematic of the gas-inlet KEMS

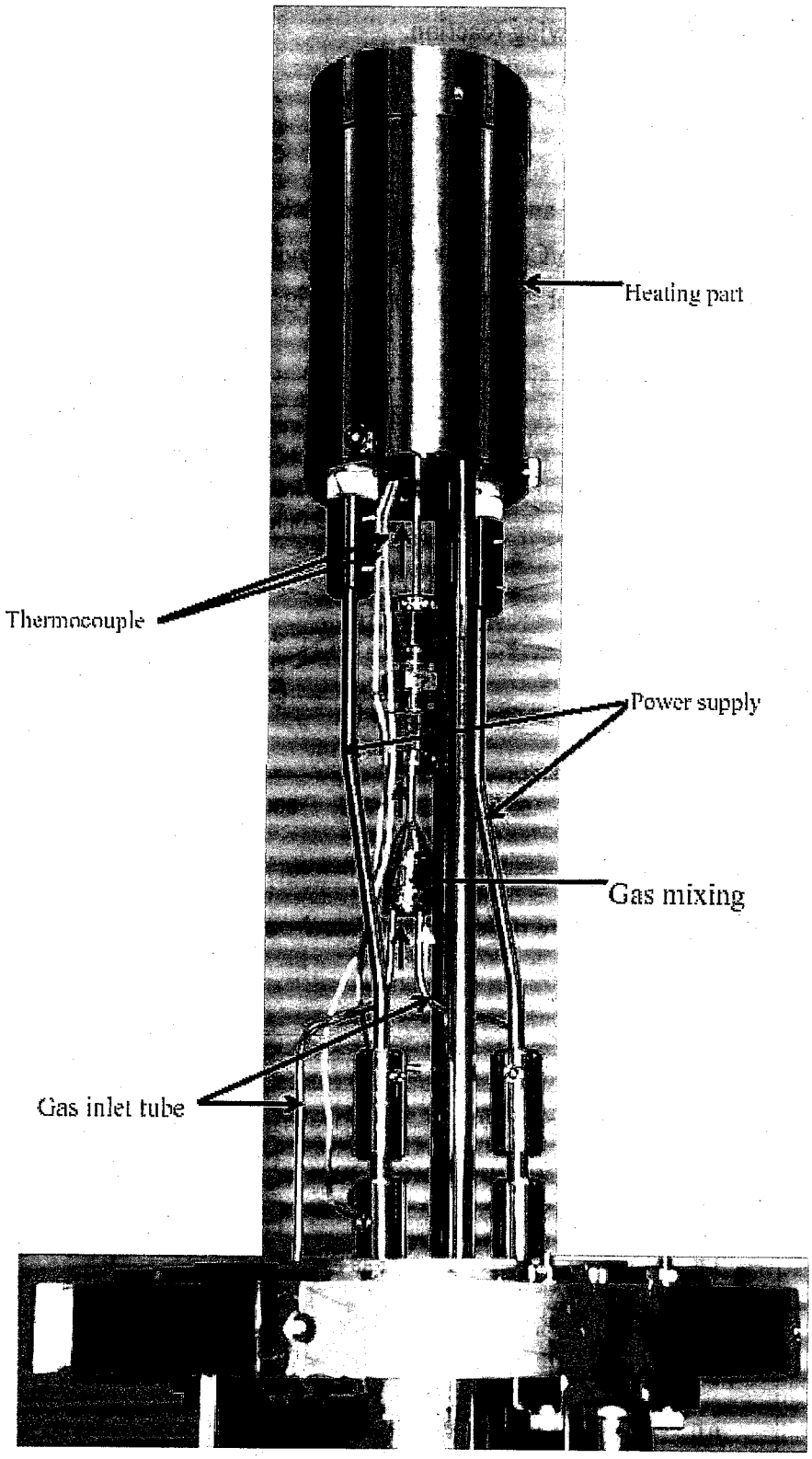

Fig. 19: The Gas-inlet system

H_2 and CO_2 were chosen as the input gases to generate water vapor and

H_2 and CO_2 were chosen as the input gases to generate water vapor and carbon dioxide environment inside the KC reactor since they could produce H_2O and CO_2 environments as the following reaction.

$$H_2 + CO_2 = CO + H_2O \quad \text{.....(13)}$$

The amounts of H_2O and CO_2 produced inside the KC can be controlled by adjusting the input ratio of H_2/CO_2. Examples of environmental condition changes in KC by inputting H_2:CO_2=1:1 or 2:1 were shown in Fig. 20-21.

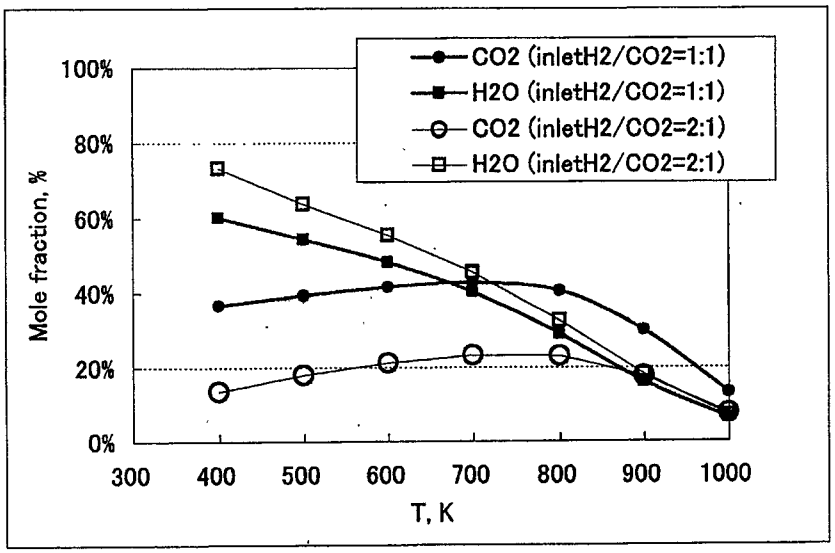

Fig. 20: Temperature dependency of environment changes in KC

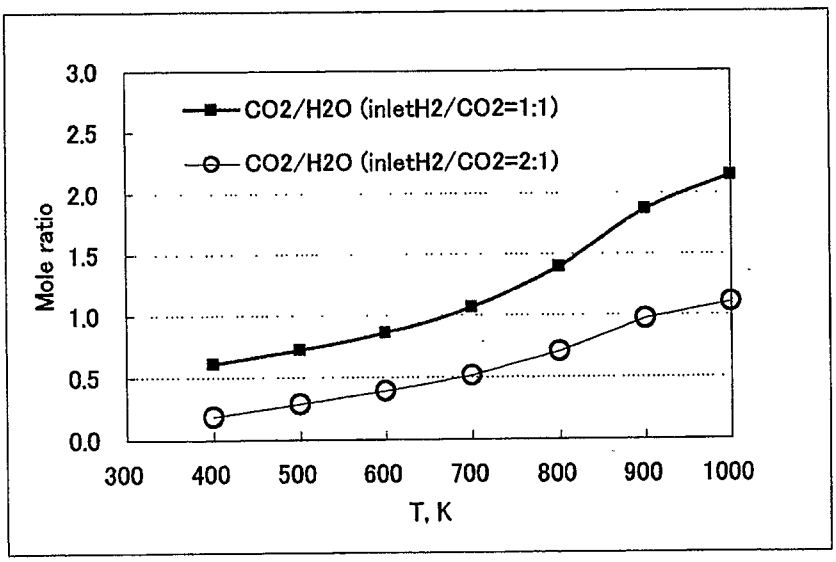

Fig. 21: Adjustment of CO_2/H_2O

Oxygen potential in the system can be obtained either from reaction $H_2O=H_2+0.5O_2$ or $CO_2 = CO + 0.5O_2$. Example results at 800 K were listed in Table 8, where 3 inlet conditions CO_2:H_2=1:1, 1:2 and 2:1were tested. Some scatter in oxygen pressure could be found for the calculation for the two reactions, but generally correct order of oxygen potential was able to be determined.

Table 8: Oxygen pressure obtained from CO_2/CO and H_2O/H_2 measured by KEMS

	Experiment1	Experiment2	Experiment3
Inlet CO_2, torr	9.4	4.6	19.2
Inlet H_2, torr	9.3	9.1	9.0
Inlet ratio CO_2:H_2	1:1	1:2	2:1
Oxygen potential obtained from reaction $CO_2=CO+0.5O_2$			
$P(O_2)$/atm	3.6E-27	1.1E-27	2.4E-26
Oxygen potential obtained from reaction $H_2O=H_2+0.5O_2$			
$P(O_2)$/atm	2.0E-27	1.9E-27	3.9E-27
Equilibrium constant of $CO_2+H_2=CO+H_2O$			
Measured Kp	0.18	0.54	0.17
Kp (by JANAF)=0.237 while averaged Kp=0.29 (measured)			

Theoretic analysis and experiments were both carried out. Introducing CO_2+H_2 mixture gas is proved to be an effective way to generate H_2O+CO_2 atmosphere inside the reaction cell of high temperature mass spectrometer. So, the effects of H_2O+CO_2 atmosphere on stability of Na-Fe oxides can be examined this way.

3.3 Sodium ferrites in H_2O/CO_2 environments by the gas-inlet KEMS

From the above theoretic calculation, it seems that carbon dioxide shows much higher influence on the stability of Na-Fe oxide than water vapor. Na_5FeO_4 was selected as the starting sodium ferrite because it should reflects the influence of water vapor and carbon dioxide shown in phase diagram Fig. 16-17. Unfortunately, the experiment result did not support the equilibrium calculation. Na_2CO_3 were only slightly formed in the surface of the sodium ferrite even if CO_2 pressure was as high as 1 Pascal level. The phases after almost 3 days testing around 1000K in H_2O+CO_2 environment were mainly Na_5FeO_4, $Na_8Fe_2O_7$ and NaOH together with a small amount of Na_2CO_3. It indicted that Na_5FeO_4 decomposed to $Na_8Fe_2O_7$ in the experimental condition instead of $NaFeO_2$ that the equilibrium calculations expected.

One possible reason could be attributed to the kinetic process because it was reported that CO_2 may require much longer time to react with sodium compounds while reaction rate of water with sodium seems very fast. Apart from the kinetic factor, the formation of Na_2CO_3 may require much more amount of CO_2 that the inlet system could supply. The gas inlet amount was limited to a molecular flow range to prevent the equilibriums inside the Knudsen cell from destruction. For this reason, introduction of water vapor and CO_2 into the KC seems not enough to result in chemical reactions with H_2O/CO_2 to a considerable extends in the gas-inlet KEMS experiments.

As a complement, a separated experiment may provide another evidence to support the above conclusions, in which a massive air including water vapor and CO_2 was sweeping over $Fe+Na_2O_2$ at flow rate of 100ml/min at 823 K. The relationship between reaction time and the products was given in Table 9. It showed that NaOH was formed since the very beginning. Na_2CO_3 was able to be identified by XRD after a few hours. It can also be noticed that the longer the reaction time, the more the content of Na_2CO_3. $NaFeO_2$ was found as the final stable sodium ferrite. At the initial stage, however, no sodium ferrites were found except for Fe_2O_3. It indicated that the Na_2CO_3 was probably formed via reaction of $NaOH+CO_2$, instead of reaction between sodium ferrites and CO_2 directly. The reason might be that the reaction speed of $NaOH+CO_2$ is much more faster. These results again suggested that reaction rate of CO_2 with sodium ferrates would be slower in orders of magnitude than other possible reaction routes.

Table 9: $Fe+Na_2O_2$ in H_2O+CO_2 at 823 K

Time (hour)	observed products
2	Na_2O_2, NaOH
4.5	Na_2O_2, NaOH, Fe_2O_3
7	NaOH, Na_2CO_3, $NaFeO_2$, Na_2O_2
20	$NaFeO_2$, Na_2CO_3, NaOH

* Products listed in order of its amount identified by the XPD analysis

Conclusion

$Na_4Fe_6O_{11}$ was prepared for crystal structure and thermodynamic analyses. One possible symmetry of was derived from its X-ray powder diffraction pattern. By using Knudsen effusion mass spectrometry, thermodynamic data were obtained, i.e., $\Delta_f H°(Na_4Fe_6O_{11})$= −3569.54±3.95 kJ·mol^{-1}, $\Delta_f G°(Na_4Fe_6O_{11})$= −3255.3±12.4 kJ·mol^{-1}, $\Delta_f G°(T)$ /J·mol^{-1} = (−3716839 ± 2274.55) + (1200.16 ± 2.35) ×T/K. It is further found that $Na_4Fe_6O_{11}$ is thermodynamically stable only at high temperatures over about 1200K. At lower temperatures, it tends to decompose into $Na_5Fe_3O_9$ or $NaFeO_2$.

From a user database of the Na-Fe-O-H-C system, equilibrium states of sodium ferrates in H_2O/CO_2 environments were calculated. Chemical potential diagrams were given as functions of P_{O2} and P_{Na}. The simulation calculation suggested that $NaFeO_2$ should be the most stable sodium ferrite together with NaOH or Na_2CO_3 depending on the atmospheres, while other sodium ferrites such as Na_5FeO_4, Na_3FeO_3 etc... would be no longer stable from the thermodynamic point of view. However, experiments by gas-inlet KEMS showed that the reaction rate of sodium ferrates with CO_2 was a time-consuming process. It suggested that actual chemical states of sodium ferrates in H_2O/CO_2 environments would be greatly affected by factors of reaction kinetics.

Acknowledgement

The authors thank Mr. K. Ohkubo for operation of the X-ray powder diffraction analysis and syntheses of the $Na_4Fe_6O_{11}$ samples.

References

1. Lindemer T. B., Besmann T. M. and Johnson C. E., J. Nucl. Mat., 100(1981)178-226.
2. Jeannot C., Malaman B., Gérardin R. and Oulladiaf B., J. Solid State Chem., 165(2002)266-277.
3. Dedushenko S. K., Kholodkovskaya L. N., et al., J. Alloys Compounds, 262-263(1997)78-80.
4. Huang Jintao, Furukawa Tomohiro and Aoto Kazumi, "Thermodynamic study of sodium-iron oxides Part I: Mass spectrometric study of Na-Fe oxides", to be published in Thermochimica Acta, 2003.
5. Huang Jintao, Furukawa Tomohiro and Aoto Kazumi, "Thermodynamic study of sodium-iron oxides Part II: Ternary phase diagram of the Na-Fe-O system", to be published in Thermochimica Acta, 2003.
6. Glasser F.P. and Potter P.E., High Temperature Chemistry of Inorganic and Ceramic Materials. The Chemical Industry:London, 1977. (Knights C.F. and Phillips B.A., 134-145.)
7. R. Collongues et J. Thery, Bull. Soc. Chim France, No. 186(1959)1141-1144.
8. Watanabe H. and Fukase M., J. Phys. Soc. Jpn., 16(1961)1181-1184.
9. Hua Shounan, Cao Gaoping and, Cui Yuezhi, J. Power Sources, 76(1998)112-115.
10. Orient O. J. and Srivastava S. K., J. Phys. B: At. Mol. Phys., B20(1987) 3923-3936.
11. Freund R. S., Wetzel R. C., Shul R. J. and Hayes T. R., Phys. Rev., A 41(1990) 3575-3595.
12. Werner P.-E., Eriksson L. and Westdahl M., J. Appl. Crystallogr., 18(1985)367-370.
13. Kale G. M. and Srikanth S., J. Am. Ceram. Soc., 83(2000)175-180.